Characterization of soluble microbial products in a partial nitrification sequencing batch biofilm reactor treating high ammonia nitrogen wastewater

Jibin Li [a], Jinglin Wei [a], Huu Hao Ngo [b], Wenshan Guo [b], Haibao Liu [a], Bin Du [a], Qin Wei [c], Dong Wei* [a]

[a] *School of Resources and Environment, University of Jinan, Jinan 250022, PR China*

[b] *School of Civil and Environmental Engineering, University of Technology Sydney, Broadway, NSW 2007, Australia*

[c] *Key Laboratory of Interfacial Reaction & Sensing Analysis in Universities of Shandong, School of Chemistry and Chemical Engineering, University of Jinan, Jinan 250022, PR China*

Abstract

In present study, the characterization of soluble microbial products (SMP) was evaluated in a partial nitrification sequencing batch biofilm reactor (SBBR). During the stable operation of SBBR, the NH_4^+-N removal efficiency and nitrite accumulation ratio were 96.70 ±0.41% and 93.77± 1.04%, respectively. According to excitation-emission matrix (EEM), the intensities of protein-like substances were reduced under anoxic and aerobic phases, whereas humic-like substances had little change during the whole cycle. Parallel factor analysis (PARAFAC) further indentified two components and their fluorescence intensity scores were both reduced. Synchronous fluorescence spectra revealed that the fluorescence intensity of protein-like fraction decreased with reaction time. Two-dimensional correlation spectroscopy (2D-COS) further demonstrated that protein-like fraction might decrease earlier than the other fractions. The information obtained in present study is of

* Corresponding author. Tel: +86 531 8276 7873; fax: +86 531 8276 7873.
E-mail address: weidong506@163.com (D. Wei).

fundamental significance for understanding the key components in SMP and their changes in partial nitrification system by using a spectral approach.

Keywords: Partial nitrification; Soluble microbial products; Parallel factor analysis; Synchronous fluorescence; Two-dimensional correlation spectroscopy.

1. Introduction

Biological nitrogen removal is commonly applied for the treatment of both domestic and industrial wastewater (Ma et al., 2016). In traditional N-removal process, ammonia is oxidized to nitrate in aerobic nitrification process and nitrate is reduced to molecular nitrogen in anoxic denitrification process (Zhou et al., 2017). As a cost-effective N-removal technology, partial nitrification has been widely developed in recent years based on the fact that nitrite is an intermediate compound in both nitrification and denitrification steps (Ciudad et al., 2005). It is generally accepted that partial nitrification via nitrite could save approximately 25% oxygen in nitrification stage and 40% carbon source in denitrification stage (Guo et al., 2009). The key control strategy to achieve partial nitrification is the enrichment of ammonia oxidizing bacteria (AOB) and limitation-inhibition-washout of nitrite oxidizing bacteria (NOB). Till now, it has been successfully achieved by appropriate regulating operational parameters, such as dissolved oxygen (DO), sludge retention time, pH value, temperature and free ammonia (FA) etc. (Ciudad et al., 2007; Peng and Zhu, 2006).

Soluble microbial products (SMP) are defined as a pool of organic compounds that are derived from the substrate metabolism (usually with biomass growth) and biomass decay during complete mineralization of supplying nutrients (Jarusutthirak and Amy, 2007). Indeed, SMP are one kind of heterogeneous mixtures containing various complex organic materials, such as proteins, polysaccharides, humic acids,

fulvic acids and organic acids etc. SMP have been drawn intensive attention in the field of wastewater treatment process due to its adverse impact on the effluent quality and treatment efficiency in wastewater treatment plant (WWTP). Many published literatures have confirmed that SMP constitute a major part of organic component in effluent from biological wastewater treatment (Wu et al., 2016; Xie et al., 2012). Additionally, some SMP may cause further environmental hazard to the receiving water after the sewage treatment systems, such as toxicity and metal chelating properties (Kunacheva et al., 2017; Liang et al., 2007). The presence of SMP may also affect the viscosity, flocculating and other physical characters of sludge (Kim et al., 2016; Zhou et al., 2009). Moreover, SMP have a certain effect on the composition changes of microbial community in bioreactor (Kunacheva and Stuckey, 2014). Hence, it is essential to clearly identify the key components of SMP for better understanding the fundamental mechanisms of biological activities. However, till now, most researches are related to the full nitrification process in activated sludge reactor, and little information is available on the production of SMP in a partial nitrification system.

To date, a series of advanced analytical methods have been applied to explore the specific components in SMP produced in biological treatment process (Guo et al., 2013). Three-dimensional excitation-emission matrix (3D-EEM) has been widely utilized for determining SMP owing to its better selectivity, higher sensitivity, and more simple and convenient operation. Combined with 3D-EEM, parallel factor analysis (PARAFAC) is commonly used to interpret the fluorescence spectra by decomposing the complete map into independent components (Zhang et al., 2016). Although PARAFAC is always applied to explore the further information of fluorescence spectra, it is not able to identify the mutual relationships between

different components (Xu and Jiang, 2013). Two-dimensional correlation spectroscopy (2D-COS) could be applied as a versatile tool to express the specific variation order of any slight changes. It has a great advantage in solving the problem of overlapping peaks occurred in the original spectra by extending the overlapped bands in second dimension (Noda, 2006). Therefore, it is of great significant to provide a comprehensive analytical method for explaining the SMP formation in partial nitrification system. However, there is little information available regarding to this point in previous literature.

Based on the above discussion, the objective of present study was to evaluate SMP production in a stable partial nitrification sequencing batch biofilm reactor (SBBR) treating high ammonia nitrogen wastewater. A spectroscopic analysis based on the combination of 3D-EEM, PARAFAC, synchronous fluorescence and 2D-COS was used to characterize SMP samples in various reaction times. The results could provide insightful information on understanding the formation of SMP in a partial nitrification system.

2. Methods and Materials

2.1. Experimental set-up

The experiment was carried out in a cylindrical SBBR with a working volume of 3.4 L. The height and inner diameter were 30 and 12 cm, respectively. Cylindrical carriers (K3, plastic media) were applied as biomass support with a packing rate of 40% (v/v). The diameter and height of each carrier were 25 and 15 mm, respectively. The specific gravity and the specific surface area of each carrier were 110 kg/m^3 and 500 m^2/m^3, respectively.

The SBBR was operated sequentially in 8h for each cycle, consisting of 5 min

for influent filling, 85 min for anoxic stage, 360 min for aeration, 15 min for settling and 15 min for effluent and idle. Aeration was provided by using an air pump and controlled through a gas flow meter. The exchange volume of SBBR was 50% for each cycle. Influent wastewater was prepared in a water tank and pumped into the bottom of biofilm system.

2.2. Synthetic wastewater and seed sludge

The influent high-strength nitrogen wastewater was shown as follows: COD (as $C_6H_{12}O_6$), 600 mg/L; NH_4^+-N (as NH_4Cl), 200 mg/L; P (as K_2HPO_4), 15 mg/L; $MgSO_4 \cdot 2H_2O$, 20 mg/L; $CaCl_2$, 40 mg/L; $FeSO_4 \cdot 2H_2O$, 20 mg/L and trace element solution 1.0 ml/L. The compositions of trace element could be found from previous literature (Tay et al., 2002). The influent pH value was adjusted to 8.0 by using $NaHCO_3$ and HCl.

Seed sludge for SBBR was collected from a lab-scale SBR of 17 L and mixed liquid suspended solids (MLSS) was controlled at about 3.0 g/L. In present study, high pH value (>8.0) and ammonia (200 mg/L) was controlled in the influent wastewater, which may provide a feasible influent FA inhibition (high of 70 mg/L) on the activity of NOB, as similarly reported in our previous literature (Wei et al., 2017). After approximately 60 days operation, partial nitrification biofilm was successfully achieved, and the biomass concentration increased to 6.0 g/L.

2.3. Fluorescence analysis

SMP samples were obtained from partial nitrification system at various reaction time from 0 to 420 min. Each sample was centrifuged at 8000 rpm for 5 min to separate out the solids. The supernatant was regarded as SMP. Fluorescence spectra were measured by using a Luminescence spectrometer (LS-55, Perkin-Elmer Co.,

USA). 3D-EEM was obtained by subsequently scanning emission from 220 to 400 nm at 10 nm increments by varying the excitation wavelength from 280 to 550 nm at 0.5 nm increments. PARAFAC analysis was obtained by using MATLAB 7.6 (Mathworks, Natick, MA, USA) with the N-way toolbox for the further analysis of EEM data (Yu et al., 2010). Synchronous fluorescence spectra were determined by ranging the excitation wavelengths from 250 to 550 nm with a constant offset ($\Delta\lambda$) of 60 nm. All samples were scanned at a speed of 1200 nm/min. 2D-COS was applied to synchronous fluorescence spectra, and detailed mathematical procedure could be found elsewhere (Noda, 2006).

2.4. Analytical methods

COD, NH_4^+-N, NO_2^--N and NO_3^--N concentrations were determined according to their respective standard methods (APHA, 2005). Total nitrogen (TN) was based on the sum of NH_4^+-N, NO_2^--N and NO_3^--N rather than an independent TN test. The DO and pH values were measured by using on-line probes (3420i, WTW Company, Germany). Nitrite accumulation ratio (NAR) of partial nitrification system was calculated according to the following equation (1) reported by Wei et al. (2015):

$$NAR\ (\%)=\frac{NO_2^-\text{-}N}{NO_2^-\text{-}N+NO_3^-\text{-}N}\times 100\% \quad (1)$$

Since the COD measurement was based on oxidation by potassium dichromate, it was influenced by nitrite (oxidized into nitrate). Thus COD values were corrected in order to estimate the oxygen demand only due to the organic substances.

$$COD=COD_{total}\text{-}COD_{nitrites}=COD_{total}-0.5(NO_2^-\text{-}N)M_{O_2}/M_N \quad (2)$$

3. Results and discussion

3.1. Performance of partial nitrification SBBR

Table 1 summarizes the contaminant removal performance of the SBBR under stable operation. The influent and effluent COD were 594.2±2.26 and 43.3±5.22 mg/L, respectively, resulting in the COD removal efficiency was high of 92.71±0.85 %. The influent NH_4^+-N concentration was kept at 190.84 ± 2.52 mg/L, while the effluent NH_4^+-N concentration was 6.29 ± 0.71 mg/L. The results implied that the removal efficiency of NH_4^+-N was high of 96.70 ±0.41% with a good nitrification performance. Nitrite was the main nitrogen species in SBBR effluent based on the fact that the presence of partial nitrification resulted in the accumulation of NO_2^--N rather than NO_3^--N. More detailed, NO_2^--N and NO_3^--N concentrations were 80.97 ± 2.53 and 5.38 ± 0.94 mg/L, respectively, resulting in a high NAR of 93.77± 1.04%. TN removal efficiency of partial nitrification SBBR was 52.67 ± 1.75%. Data implied that a better nitrogen removal performance in partial nitrification SBBR was obtained under stable operation.

Fig.1 shows the variations of nitrogen compound, DO and pH values in partial nitrification SBBR during one typical cycle. As shown in Fig. 1A, the decrease of NH_4^+-N and NO_2^--N concentrations were mainly attributed to dilution and pre-denitrification in anoxic stage (5-90 min). In aeration stage (90-450 min), NH_4^+-N concentration significantly decreased from 97.44 to 6.12 mg/L, whereas NO_2^--N concentration increased from 0.70 to 80.16 mg/L. Moreover, there was no obvious accumulation of NO_3^--N during the whole typical cycle. Although the DO concentration was maintained at about 6 mg/L in aerobic stage (Fig. 1B), high NAR (93.77±1.04%) was observed in the effluent. And the detailed inhibition mechanism might due to the co-existence of free ammonia (FA) and free nitrous acid (FNA), as similarly reported by Wei et al (2014). Additionally, pH value gradually decreased

168 from 8.62 to 8.08 and next increased to 8.24 during aeration stage. The reason might
169 be based on the fact that ammonium was converted to nitrite, which led to the increase
170 of hydrogen ion concentration. After that, the increase in pH values might be due to
171 the completion of nitrification and the stripping of carbon dioxide (Peng and Zhu,
172 2006; Wei et al., 2017).

173 ***3.2. 3D-EEM spectra***

174 Fig. 2 shows the 3D-EEM spectra of SMP samples corresponding to reaction
175 time in a typical cycle. According to the sampling time, Fig. 2A represented the SMP
176 sample after influent filling, whereas Fig. 2B-D and Fig. 2E-I represented for anoxic
177 and aeration stage, respectively. It was found that three major peaks (Peak A, B, C)
178 were indentified in the SMP spectra. Peak A was observed at the excitation/emission
179 (Ex/Em) wavelengths of 280/350 nm, which was related to tryptophan protein-like
180 substances. Peak B and Peak C were located at Ex/Em of 230/335-355 nm and
181 330-350/420-431 nm, which represented aromatic protein-like substances and
182 humic-like substances, respectively (Chen et al., 2003).

183 It was clearly observed that Peak A and Peak B in Fig. 2A had the highest
184 fluorescence intensities, and generally decreased with different trends to reaction time,
185 in despite of anoxic and aerobic stages. The rapid SMP formation at 5 min suggested
186 that the influent stimulated activated microorganism led to the release of SMP (Fig.
187 2A). Afterwards, the fluorescence intensities of peak A and peak B significantly
188 decreased from 470.59 and 770.09 a.u. to 319.30 and 463.78 a.u. at 90 min,
189 respectively. Therefore, protein-like substances in SMP may be utilized as carbon
190 source for microbial denitrification process. At subsequent aerobic stage, the intensity
191 of Peak A generally reduced to 112.07 a.u. at 420 min, whereas Peak B was generally
192 disappeared at 120 min. The changes in Peak A and Peak B intensities suggested that

193 protein-like substances may be easily bio-degradable during aerobic condition, as
194 similarly reported by Wu et al. (2016). In contrast, the intensity of peak C had little
195 change during the typical cycle. Previous literature has been reported that humic-like
196 substances were representative of the non-biodegradable component (Wang et al.,
197 2009). Moreover, an obvious blue-shift in terms of emission wavelength was observed
198 in Peak A, implying the changed chemical composition during nitrogen treatment
199 process

200 ***3.3. PARAFAC analysis***

201 PARAFAC could decompose complex EEM data into independent fluorescence
202 components, which represent groups of similar fluorophores (Ishii and Boyer, 2012).
203 It was found from PARAFAC model that the fluorescent SMP samples from partial
204 nitrification system could be indentified into two components (Fig.3). Two peaks were
205 exhibited in component 1 (Ex/Em of 280/342.5 nm and Ex/Em of 230/342.5 nm),
206 which were corresponded to tryptophan protein-like substances and aromatic
207 protein-like substances, respectively (Phong and Hur, 2015). Component 2 was
208 characterized three main peaks that represented the presence of humic-like substances
209 (Ex/Em of 350/427 nm and 250/433 nm) and fulvic-like substances (Ex/Em of
210 220/433 nm) (Wu et al., 2011).

211 PARAFAC also provides additional information to quantitatively describe the
212 variations of two components, as displayed in Fig. 4. It was found that the
213 fluorescence intensity scores of the two components decreased from 0.67 and 0.66 to
214 0.06 and 0.17 during the typical cycle, respectively. In addition, the decreased degree
215 of component 1 was greater than that of component 2, indicating that protein-like
216 substances changed to a much higher extent than those of humic-like substances and
217 fulvic-like substances. PARAFAC coupled with 3D-EEM has been widely used to

characterize SMP or DOM in wastewater treatment process. Sanchez et al. (2013) found that the loadings of PARAFAC sample exhibited a higher association with the total EEM signal in the raw and treated water samples compared with alternative analysis techniques. The study reported by Ou et al. (2014) indicated that EEM-PARAFAC not only can rapidly identify fluorescent matter characteristics, but also can indirectly reflect the variations of representative contaminants. The analysis results showed that EEM-PARAFAC could be used as a promising monitoring tool for tracking the trends of fluorescence components in a partial nitrification process.

3.4. Synchronous fluorescence spectra

Synchronous fluorescence spectra have the advantages of higher selectivity and sensitivity in the assessment of multi-component materials. As shown in Fig. 5, three fluorescence regions (protein-like, fulvic-like and humic-like fractions) could be assigned to the wavelength ranges of 250-300, 300-380 and 380-550 nm, respectively (Chen et al., 2015). The data showed that the fluorescence intensity of SMP samples gradually decreased in the whole range of wavelengths with the reaction time from 0 to 420 min. In addition, a major peak corresponding to protein-like fluorescence fraction was identified at the wavelength of 260 nm. The observation of protein-like fluorescence fraction as the main component in SMP was consistent with the evaluation of 3D-EEM.

3.5. 2D-COS

In order to resolve the overlapping peaks problem, 2D-COS was conducted to enhance the spectral resolution by distributing spectral intensity trends over a second dimension. In synchronous 2D-COS map (Fig. 6A), one positive auto-peak along the diagonal line was identified at 282 nm, suggesting that protein-like fraction was more susceptible than other fractions. All peaks identified from synchronous 2D-COS map

are positive, indicating that the decrease of fluorescence intensity proceed in the same direction, as similarly with the observation reported by Hur and Lee (2011).

Asynchronous 2D-COS map was used to determine the response order of different molecules or groups along a given external perturbation. As shown in Fig. 6B, two main positive cross-peaks at 291/349.5, 291/366 nm and two negative cross-peaks at 264/291, 282.5/291 nm were observed upper the diagonal line of asynchronous map. According to Noda's rule (2005), the variation of fluorescence to reaction time took place sequentially in the order: 264 and 282.5>291>349.5 and 366 nm. The results demonstrated that protein-like fraction might occur earlier than the other fractions.

4. Conclusions

In summary, a partial nitrification lab-scale SBBR was achieved by controlling the influent high pH value and NH_4^+-N. It was found that the reactor expressed better organic matter and nitrogen removal efficiencies during stable operation. A combined use of EEM, PARAFAC, synchronous fluorescence and 2D-COS was conducted to characterize SMP samples in the typical cycle of partial nitrification system. EEM-PARAFAC indentified three fluorescence peaks and two components in SMP samples. Synchronous fluorescence spectra and 2D-COS analysis demonstrated that protein-like fraction was the dominant components in SMP and took place earlier than the other fractions with reaction time.

Acknowledgments

This study was supported by the Natural Science Foundation of Chinese (21377046), Natural Science Foundation of Shan dong Province (ZR201702070162), the Special Project of Independent Innovation and Achievements Transformation of

Shandong Province (2014ZZCX05101), the Science and Technology Development Plan Project of Shandong Province (2014GGH217006), and QW thanks the Special Foundation for Taishan Scholar Professorship of Shandong Province and UJN (No. ts20130937).

References

[1] APHA, AWWA, WEF. 2005. Standards methods for the examination of water and wastewater. 21st ed. Washington, D.C.

[2] Chen, W., Habibul, N., Liu, X.Y., Sheng, G.P., Yu, H.Q. 2015. FTIR and synchronous fluorescence heterospectral two-dimensional correlation analyses on the binding characteristics of copper onto dissolved organic matter. *Environ Sci Technol*.**49**(4), 2052-8.

[3] Chen, W., Westerhoff, P., Leenheer, J.A., Booksh, K. 2003. Fluorescence excitation-emission matrix regional integration to quantify spectra for dissolved organic matter. *Environ Sci Technol.* **37**(24), 5701.

[4] Ciudad, G., Gonzalez, R., Bornhardt, C., Antileo, C. 2007. Modes of operation and pH control as enhancement factors for partial nitrification with oxygen transport limitation. *Water Res*. **41**(20), 4621-9.

[5] Ciudad, G., Rubilar, O., Muñoz, P., Ruiz, G., Chamy, R., Vergara, C., Jeison, D. 2005. Partial nitrification of high ammonia concentration wastewater as a part of a shortcut biological nitrogen removal process. *Process Biochemistry*. **40**(5), 1715-1719.

[6] Guo, J., Peng, Y., Wang, S., Zheng, Y., Huang, H., Wang, Z. 2009. Long-term effect of dissolved oxygen on partial nitrification performance and microbial community structure. *Bioresour Technol*. **100**(11), 2796-2802.

[7] Guo, X.J., Yuan, D.H., Jiang, J.Y., Zhang, H., Deng, Y. 2013. Detection of dissolved organic matter in saline-alkali soils using synchronous fluorescence spectroscopy and principal component analysis. *Spectrochim Acta A Mol Biomol Spectrosc*. **104**, 280-6.

[8] Hur, J., Lee, B.M. 2011. Characterization of binding site heterogeneity for copper within dissolved organic matter fractions using two-dimensional correlation fluorescence spectroscopy. *Chemosphere*. **83**(11), 1603-11.

[9] Ishii, S.K., Boyer, T.H. 2012. Behavior of reoccurring PARAFAC components in fluorescent dissolved organic matter in natural and engineered systems: a critical review. *Environ Sci Technol*. **46**(4), 2006-17.

[10] Jarusutthirak, C., Amy, G. 2007. Understanding soluble microbial products (SMP) as a component of effluent organic matter (EfOM). *Water Res*. **41**(12), 2787-93.

[11] Kim, N.K., Oh, S., Liu, W.T. 2016. Enrichment and characterization of

microbial consortia degrading soluble microbial products discharged from anaerobic methanogenic bioreactors. *Water Res*. **90**, 395-404.

[12] Kunacheva, C., Soh, Y.N.A., Stuckey, D.C. 2017. Effect of feed pH on Reactor Performance and Production of Soluble Microbial Products (SMPs) in a Submerged Anaerobic Membrane Bioreactor. *Chem. Eng. J*.

[13] Kunacheva, C., Stuckey, D.C. 2014. Analytical methods for soluble microbial products (SMP) and extracellular polymers (ECP) in wastewater treatment systems: a review. *Water Res*. **61**, 1-18.

[14] Liang, S., Liu, C., Song, L. 2007. Soluble microbial products in membrane bioreactor operation: Behaviors, characteristics, and fouling potential. *Water Res*. **41**(1), 95-101.

[15] Ma, B., Wang, S., Cao, S., Miao, Y., Jia, F., Du, R., Peng, Y. 2016. Biological nitrogen removal from sewage via anammox: Recent advances. *Bioresour Technol*. **200**, 981-90.

[16] Noda, I. 2006. New Approaches to Generalized Two-Dimensional Correlation Spectroscopy and Its Applications. *Applied Spectroscopy Reviews*. **41**(5), 515-547.

[17] Noda, I., Ozaki, Y. 2005. *Two-Dimensional Correlation Spectroscopy - Applications in Vibrational and Optical Spectroscopy*.

[18] Ou, H.S., Wei, C.H., Mo, C.H., Wu, H.Z., Ren, Y., Feng, C.H. 2014. Novel insights into anoxic/aerobic(1)/aerobic(2) biological fluidized-bed system for coke wastewater treatment by fluorescence excitation-emission matrix spectra coupled with parallel factor analysis. *Chemosphere*. **113**, 158-64.

[19] Peng, Y., Zhu, G. 2006. Biological nitrogen removal with nitrification and denitrification via nitrite pathway. *Appl Microbiol Biotechnol*. **73**(1), 15-26.

[20] Phong, D.D., Hur, J. 2015. Insight into photocatalytic degradation of dissolved organic matter in UVA/TiO2 systems revealed by fluorescence EEM-PARAFAC. *Water Res*. **87**, 119-126.

[21] Sanchez, N.P., Skeriotis, A.T., Miller, C.M. 2013. Assessment of dissolved organic matter fluorescence PARAFAC components before and after coagulation-filtration in a full scale water treatment plant. *Water Res*. **47**(4), 1679-90.

[22] Tay, J.H., Liu, Q.S., Liu, Y. 2002. Characteristics of aerobic granules grown on glucose and acetate in sequential aerobic sludge blanket reactors. *Environmental Technology*. **23**(8), 931-936.

[23] Wang, Z., Wu, Z., Tang, S. 2009. Characterization of dissolved organic matter in a submerged membrane bioreactor by using three-dimensional excitation and emission matrix fluorescence spectroscopy. *Water Res*, **43**(6). 1533-40.

[24] Wei, D., Du, B., Zhang, J., Hu, Z., Liang, S., Li, Y. 2015. Composition of extracellular polymeric substances in a partial nitrification reactor treating high ammonia wastewater and nitrous oxide emission. *Bioresour Technol*, **190**, 474-9.

[25] Wei, D., Xue, X., Yan, L., Sun, M., Zhang, G., Shi, L., Du, B. 2014. Effect of influent ammonium concentration on the shift of full nitritation to partial nitrification in a sequencing batch reactor at ambient temperature. *Chem. Eng. J.* **235**, 19-26.

[26] Wei, D., Zhang, K., Ngo, H.H., Guo, W., Wang, S., Li, J., Han, F., Du, B., Wei, Q. 2017. Nitrogen removal via nitrite in a partial nitrification sequencing batch biofilm reactor treating high strength ammonia wastewater and its greenhouse gas emission. *Bioresour Technol.* **230**, 49-55.

[27] Wu, J., Zhang, H., He, P.J., Shao, L.M. 2011. Insight into the heavy metal binding potential of dissolved organic matter in MSW leachate using EEM quenching combined with PARAFAC analysis. *Water Res.* **45**(4), 1711-9.

[28] Wu, N., Wei, D., Zhang, Y., Xu, W., Yan, T., Du, B., Wei, Q. 2016. Comparison of soluble microbial products released from activated sludge and aerobic granular sludge systems in the presence of toxic 2,4-dichlorophenol. *Bioprocess & Biosystems Engineering*. 1-10.

[29] Xie, W.M., Ni, B.J., Seviour, T., Sheng, G.P., Yu, H.Q. 2012. Characterization of autotrophic and heterotrophic soluble microbial product (SMP) fractions from activated sludge. *Water Res.* **46**(19), 6210-7.

[30] Xu, H., Jiang, H. 2013. UV-induced photochemical heterogeneity of dissolved and attached organic matter associated with cyanobacterial bloomsina eutrophic freshwater lake. *Water Res.* **47**(17), 6506-15.

[31] Yu, G.H., Luo, Y.H., Wu, M.J., Tang, Z., Liu, D.Y., Yang, X.M., Shen, Q.R. 2010. PARAFAC modeling of fluorescence excitation-emission spectra for rapid assessment of compost maturity. *Bioresour Technol*, **101**(21). 8244-51.

[32] Zhang, S., Chen, Z., Wen, Q., Zheng, J. 2016. Assessing the stability in composting of penicillin mycelial dreg via parallel factor (PARAFAC) analysis of fluorescence excitation–emission matrix (EEM). *Chem. Eng. J.* **299**, 167-176.

[33] Zhou, W., Wu, B., She, Q., Chi, L., Zhang, Z. 2009. Investigation of soluble microbial products in a full-scale UASB reactor running at low organic loading rate. *Bioresour Technol.* **100**(14), 3471-6.

[34] Zhou, X., Wang, X., Zhang, H., Wu, H. 2017. Enhanced nitrogen removal of low C/N domestic wastewater using a biochar-amended aerated vertical flow constructed wetland. *Bioresour Technol.* **241**, 269-275.

382

383 **Figure capations**

384 **Fig. 1** Variations of nitrogen compound, DO and pH values in partial nitrification
385 SBBR during one typical cycle.

386 **Fig. 2** 3D-EEM spectra of SMP samples corresponding to reaction time in typical
387 cycle: (A) 5 min; (B) 30 min;(C) 60 min; (D) 90 min; (E) 120 min; (F) 150 min; (G)
388 210 min; (H) 330 min. (I) 420 min.

389 **Fig. 3** Fluorescence components of SMP samples identified by PARAFAC based on
390 EEM spectra: (A) Component 1(B) Component 2.

391 **Fig. 4** Fluorescence intensity scores of two PARAFAC-derived components in SMP
392 samples.

393 **Fig. 5** Changes in synchronous fluorescence spectra of SMP corresponding to reaction
394 time.

395 **Fig. 6** Synchronous (A) and asynchronous (B) 2D-COS maps from synchronous
396 fluorescence spectra.

397

398

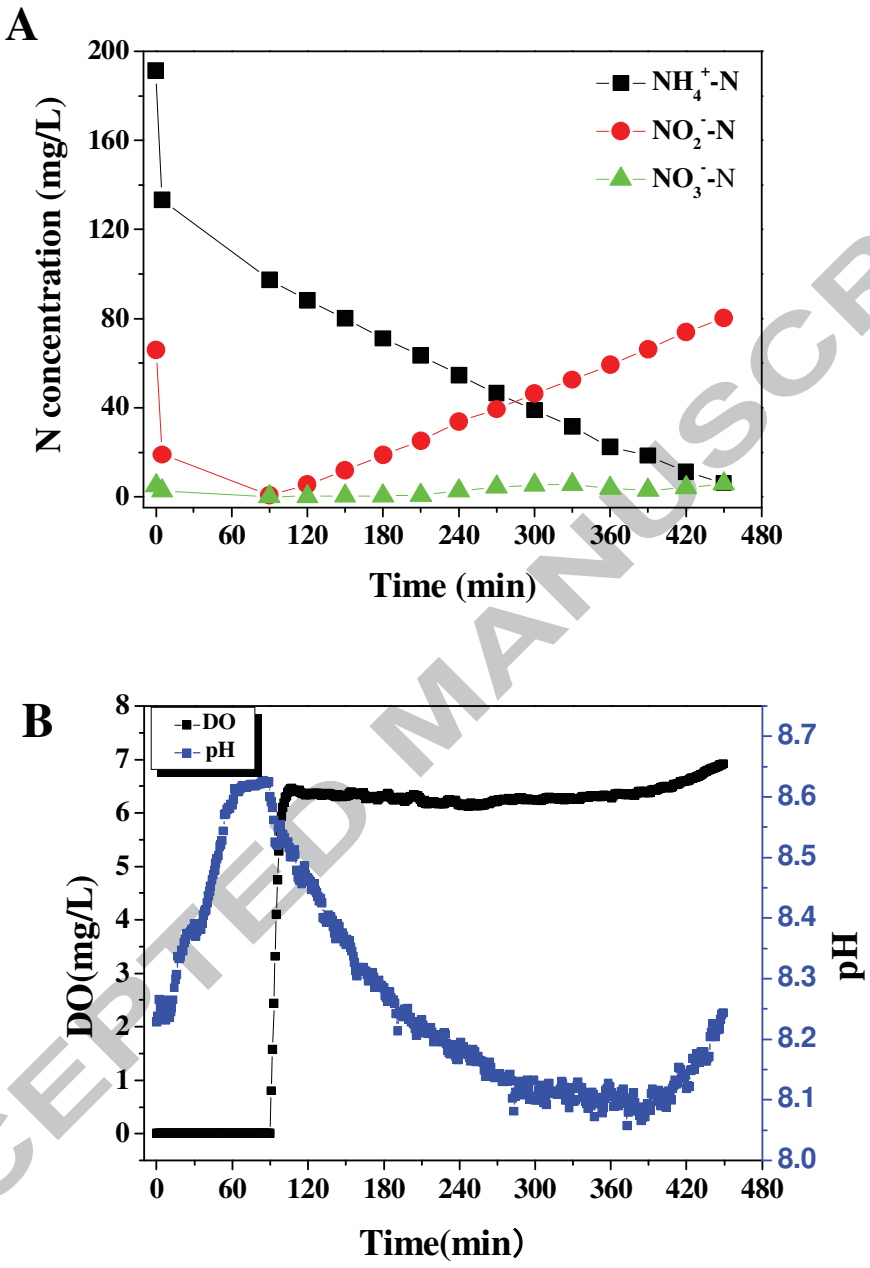

399

400 **Fig. 1** Variations of nitrogen compound, DO and pH values in partial nitrification

401 SBBR during one typical cycle.

402

403

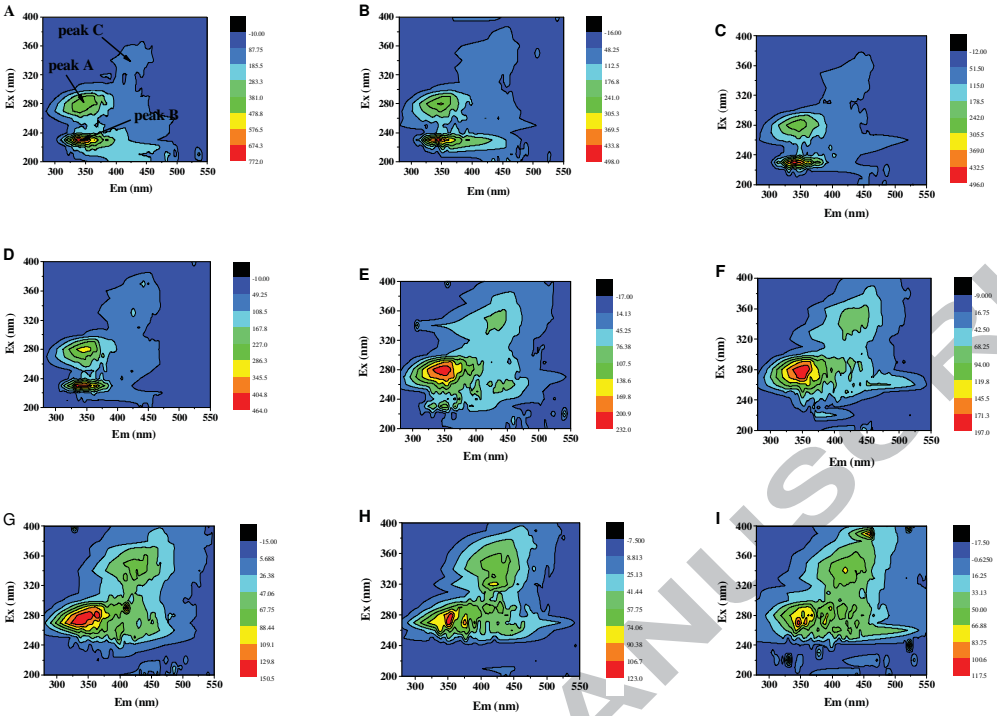

404

405 **Fig. 2** 3D-EEM spectra of SMP samples corresponding to reaction time in typical

406 cycle: (A) 5 min; (B) 30 min;(C) 60 min; (D) 90 min; (E) 120 min; (F) 150 min; (G)

407 210 min; (H) 330 min. (I) 420 min.

408

409

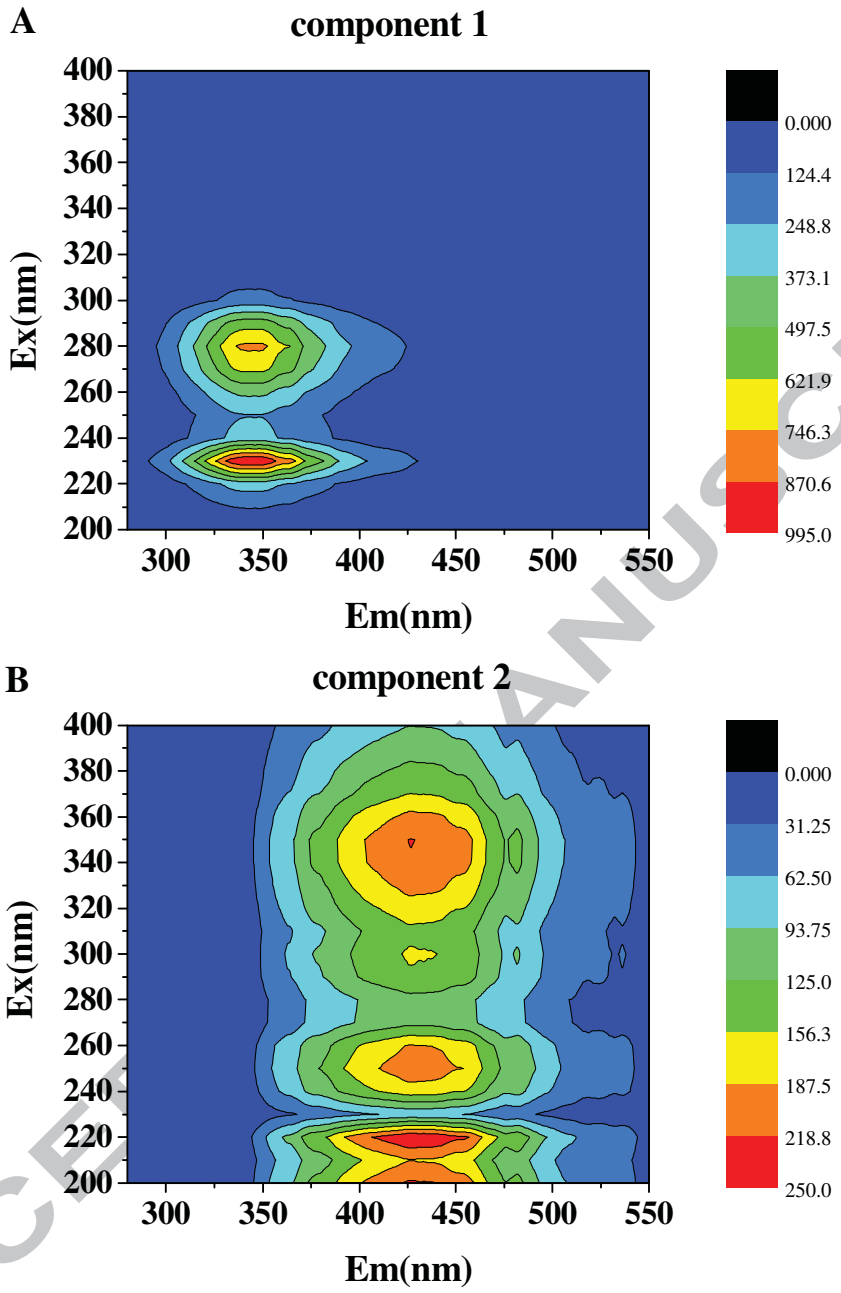

410

411 **Fig. 3** Fluorescence components of SMP samples identified by PARAFAC based on

412 EEM spectra: (A) Component 1(B) Component 2.

413

414

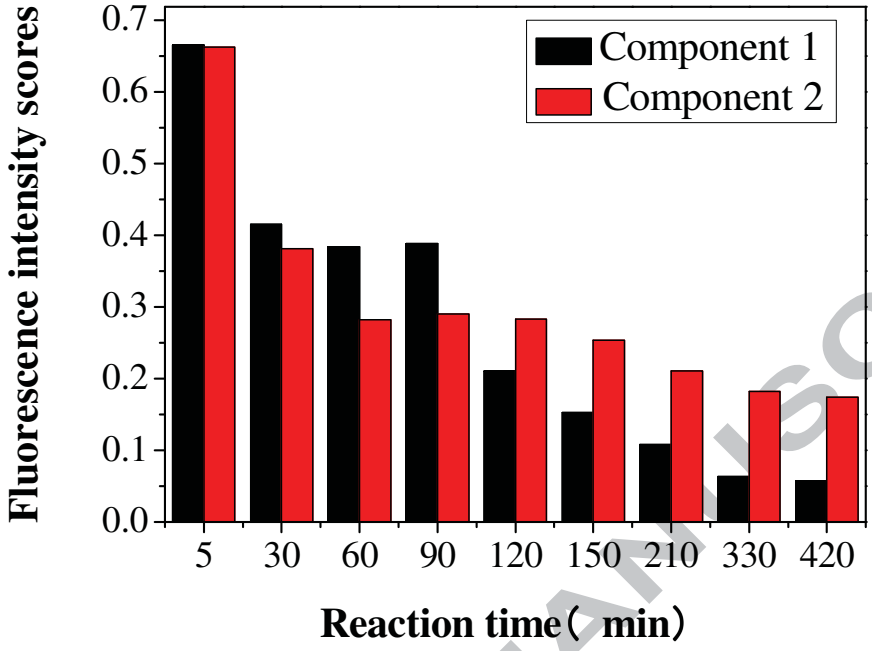

415

416 **Fig. 4** Fluorescence intensity scores of two PARAFAC-derived components in SMP

417 samples.

418

419

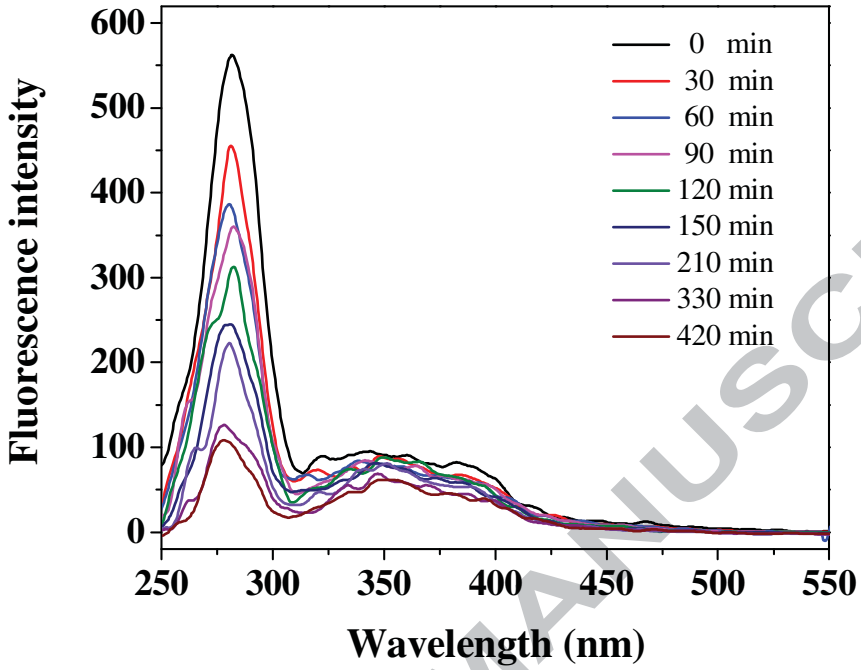

420

421 **Fig. 5** Changes in synchronous fluorescence spectra of SMP corresponding to reaction

422 time.

423

424

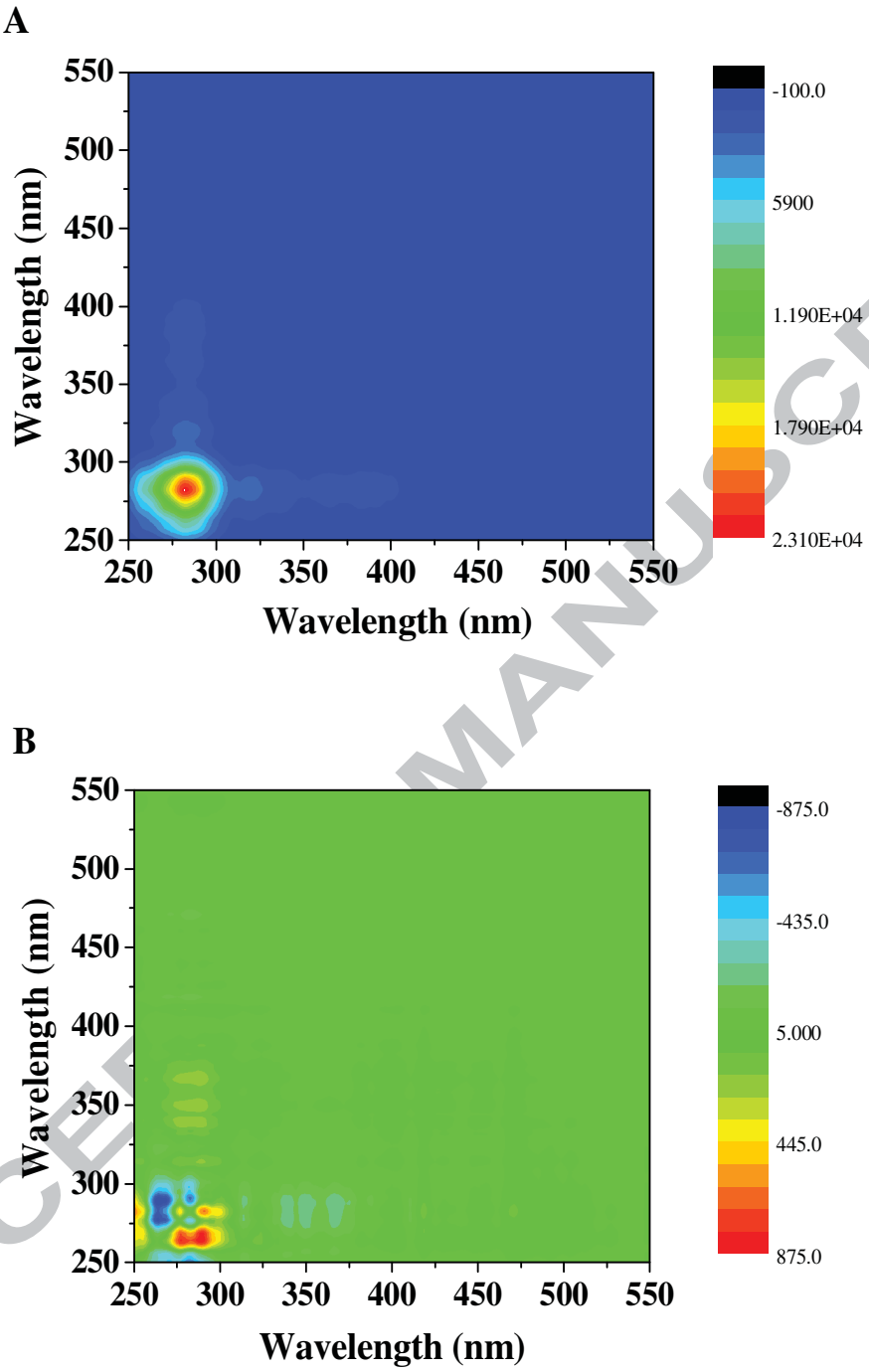

425

426 **Fig. 6** Synchronous (A) and asynchronous (B) 2D-COS maps from synchronous

427 fluorescence spectra.

428

429 **Table.1** The contaminant removal performance of SBBR under stable operation.

Parameters	Influent (mg/L)	Effluent (mg/L)	Removal Efficiency (%)
COD	594.2±2.26	43.3±5.22	92.71±0.85
NH_4^+-N	190.84±2.52	6.29±0.71	96.70±0.41
NO_2^--N		80.97±2.53	
NO_3^--N	4.94±0.24	5.38±0.94	
TN	195.78±2.71	92.64±2.75	52.67±1.75
NAR (%)		93.77±1.04	

430

431

432